절연형 단상 태양광 PCS의 직류링크 커패시터 저감

누옌황부, 이동춘
영남대학교 전기공학과

Reduction of DC-link Capacitance for Single-Phase Transformerless Photovoltaic Power Converters

Hoang Vu Nguyen, Dong-Choon Lee
Department of Electrical Engineering, Yeungnam University

ABSTRACT

This paper presents a single-phase transformerless photovoltaic (PV) power converter systems based on the AC/DC boost inverter, which is capable of solving the leakage current and second-order ripple power issues. By eliminating the inherent ripple power in single-phase inverter, the bulky electrolytic capacitor can be replaced by a small film capacitor. The validity of the proposed scheme has been verified by the simulation results.

1. Introduction

Nowadays, grid-connected PV system, particularly low-power transformerless single-phase PV systems become more important in field applications. In this system, the leakage current may flow due to lack of galvanic isolation, which should be carefully handled to comply with the standard. So, many topologies have been proposed to eliminate the leakage current in transformerless single-phase PV systems [1]. However, in these systems, additional devices are required, which increases the system complexity, cost, and power losses.

Beside the leakage current issue, there is a critical problem of second-order ripple power in single-phase inverter. Normally, bulky electrolytic capacitors are usually used to absorb this pulsating power so that the DC voltage is kept at a relatively constant. This, however, results in a large converter size, consequently, low power density. In recent time, a large of active method is suggested to reduce the DC-link capacitance requirement, hence the film capacitors can be used instead of electrolytic capacitors [2]. Unfortunately, the auxiliary circuit with active components is required, which increases the power losses, cost and the complexity of the system. In [3], the boost DC-AC inverter is presented for fuel-cell systems, in which the second-order current ripple in DC side can be reduced.

In this paper, a single-phase transformerless PV power converter based on boost DC-AC inverter is proposed, which can suppress the leakage current remarkably without any additional components. Also, by properly controlling the capacitor voltages, the pulsating power component can be absorbed by the two output capacitors of the inverter, thereby minimizing the DC-link capacitor. Therefore, the film capacitors can be adopted instead of using electrolytic capacitor. The validity of the proposed scheme is verified by simulation results.

2. Circuit Configuration and Control Scheme

2.1 Single-phase transformerless PV power converter systems

The configuration of single-phase transformerless PV power converter systems is shown in Fig. 1. The inverter consists of two bidirectional boost converter, where their output terminals are connected in series. The output voltage of the boost inverter is given by

$$v_0 = v_s = V_s \sin(\omega t) \quad (1)$$

where V_s is the rms values of the input voltage and ω is the line angular frequency.

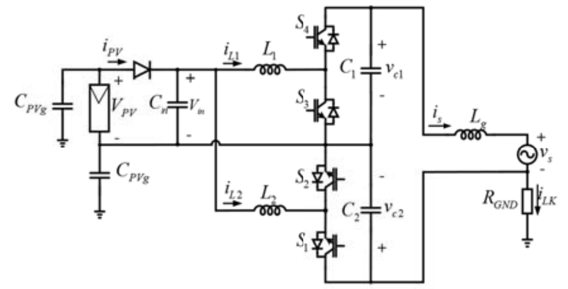

Fig. 1. A single-phase transformerless grid-connected PV system.

Voltages across the output capacitors C_1 and C_2 are required to follow their references v_{01_ref} and v_{02_ref} given by (2) and (3), respectively, in order to achieve the required output voltage

$$v_{01\_ref} = V_d + \frac{V_s}{2}\sin(\omega t) \quad (2)$$

$$v_{02\_ref} = V_d - \frac{V_s}{2}\sin(\omega t) \quad (3)$$

where $V_d > V_{in} + \frac{V_s}{2}$ is the offset in the output capacitor voltages.

It is assumed that the input current is sinusoidal as $i_s = I_s \sin(\omega t)$. Then, the instantaneous input power is

$$p_s = V_s \sin(\omega t) \times I_s \sin(\omega t) = \frac{V_s I_s}{2} - \frac{V_s I_s}{2}\cos(2\omega t). \quad (4)$$

It can be seen that there is an inherent pulsating power in single-phase system, which is reflected in the $\cos(2\omega t)$ term. In order to decouple the double-line-frequency component in (4), the upper and lower capacitor voltages need to be modified, respectively, as

$$v_{01\_ref} = V_d + \frac{V_s}{2}\sin(\omega t) + B\sin(\omega t + \delta) \quad (5)$$

$$v_{02\_ref} = V_d - \frac{V_s}{2}\sin(\omega t) + B\sin(\omega t + \delta) \quad (6)$$

where the amplitude, B, and the phase angle, δ, of the compensated components is derived as

$$\mathrm{B} = \frac{V_s}{8V_d\omega C}\sqrt{I_s^2 + \omega^2 C^2 V_s^2 / 4} \quad (7)$$

$$\delta = \frac{\tau}{2} - \sin^{-1}\frac{I_s}{\sqrt{I_s^2 + \omega^2 C^2 V_s^2 / 4}} \quad (8)$$

2.2 Proposed control method for PV power converter system

Fig. 2 shows the control block diagram of the PV power converter systems. The MPPT control method using P&O (perturb and observe) algorithm is adopted to extract the maximum power produced in PV system. Next, the phase-lock-loop is used to provide a unity power factor operation which involves synchronization of the inverter output current with the grid voltage. To achieve the sinusoidal input

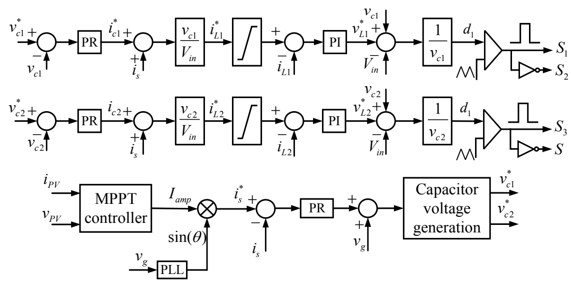

Fig. 2. Control block diagram of PV power converter systems

TABLE I. PARAMETERS OF PV POWER CONVERTER SYSTEMS

Parameters	Symbol	Value
Power rating	P_n	600W
Grid voltage	V_s	220 V (RMS), 60 Hz
PV voltage	V_{MPP}	168 V
Grid inductance	L_g	500μH
Output capacitance	C_1, C_2	70 μF
DC-link capacitance	C_{in}	50 μF
Input inductance	L_1, L_2	500 μH
Switching frequency	f_{sw}	20 kHz
Parasitic capacitance	C_{PVg}	110nF
Ground resistance	R_{GND}	10Ω

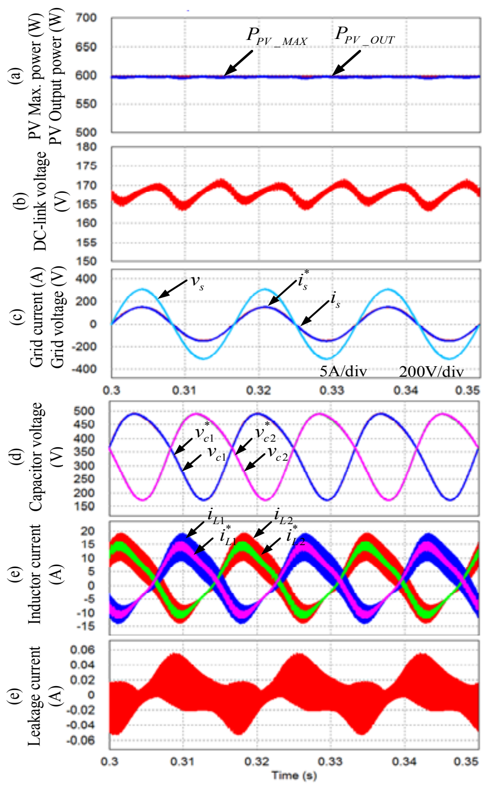

Fig. 3. Control performance of PV system at rated power condition. (a) PV maximum power and PV output power. (b) DC-link voltage. (c) Grid current and grid voltage. (d) Capacitor voltage. (e) Inductor current. (f) Leakage current.

current, the proportional-resonant (PR) controller is adopted to control the grid current. The output of the current controller is used to generate the voltage references of the upper and lower capacitors, which is shown in (5) and (6), respectively. In addition, the dual-loop controllers are used to control the boost inverter, where each double-loop controller has an inner current control loop and an outer voltage control loop. The PI controller is applied to control the inductor currents, while the PR controller is adopted to regulate the capacitor voltages.

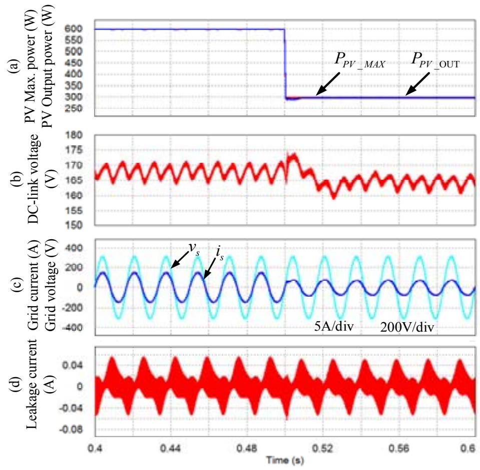

Fig. 4. Responses at a stepwise decrease of solar irradiance. (a) PV maximum power and PV output power. (b) DC-link voltage. (c) Grid current and grid voltage. (d) Leakage current.

3. Simulation Results

To verify the effectiveness of the proposed circuit, the PSIM tool has been used to carry out the simulation test for 600 W PV power converter system. The system parameters are listed in Table I. It should be noted that only 50 μF capacitor is used in the DC-link.

Fig. 3 shows the control performance of the PV power converter system at steady condition, in which the system is operated at rated power with a solar irradiance of 10 kW/m2. It can be seen from Fig. 3(a) that the output power accurately tracks the maximum power produced in PV system. The DC-link voltage is shown in Fig. 3(b), where the ripple is about 3% compared with the MPP voltage value of 168 V. Also, the grid current is controlled to be sinusoidal at unity power factor, as shown in Fig. 3(c). The capacitor output voltages are shown in Fig. 3(d), in which the actual voltages are regulated toward the references. Fig. 3(e) shows the inductor currents, which are kept closely to their references. As shown in Fig. 3(f), the leakage current is very low, where its rms value is about 21 mA. It is far below the limit of 300 mA.

The dynamic response of the system is shown in Fig. 4, when the irradiation is suddenly changed from 1 kW/m2 to 0.5 kW/m2. It can be seen that the whole system is kept stable. The leakage current of the PV system is shown in Fig. 4(d), where it is always in a very low level.

5. Conclusions

In this paper, a single-phase transformerless PV power converter system has been presented, in which the leakage current can be eliminated without any additional devices. In addition, the inherent pulsating power in single-phase PV inverter has been also solved by modifying the capacitor voltage waveforms so that this pulsation component is absorbed by two output capacitors. Therefore, a small film capacitor can replace the bulky electrolytic capacitor. The effectiveness of the proposed topology has been verified by simulations results.

Acknowledgment

This research was supported by the National Research Foundation of Korea (NRF) grant funded by the Korea government (MSIP) (No. 2014R1A2A1A11052748).

References

[1] W. Li, Y. Gu, H. Luo, W. Cui, X. He, and C. Xia, “Topology review and derivation methodology of single-phase transformerless photovoltaic inverters for leakage current suppression,” *IEEE Trans. Ind. Electron.*, vol. 62, no. 7, pp. 4537–4551, Jul. 2015.

[2] H. Hu, S. Harb, N. Kutkut, I. Batarseh, and Z. J. Shen, “A review of power decoupling techniques for microinverters with three different decoupling capacitor locations in PV systems,” *IEEE Trans. Power Electron.*, vol. 28, no. 6, pp. 2711–2726, 2013.

[3] G. R. Zhu, S. C. Tan, Y. Chen, and C. K. Tse, “Mitigation of low-frequency current ripple in fuel-cell inverter systems through waveform control,” *IEEE Trans. Power Electron.*, vol. 28, no. 2, pp. 779–792, 2013.